

In Figure 3 the outputs of PAMKE and FAMKE are the same for $\text{Re}\beta > -0.37$. At this point the convergence test fails and FAMKE then calculates the attenuation for one less knife-edge (the portion of the dashed curve labeled $N_{\text{eff}} = 4$). Similar failures occur at -0.42 and -0.62 , resulting in the discontinuities at these values. It can be seen that differences in attenuation from the exact curve as calculated by PAMKE are always less than 1.5 dB.

The partitioning procedure described in this section provides a means of calculating the MKE attenuation function (equation (28)) for any knife-edge heights without concern for the problems of discontinuities or significant figure loss. Details of attenuation variation even in the interference region can thus be shown for any combination of knife-edges.

4. DISCUSSION

The derivation of the MKE function by Fresnel-Kirchhoff theory as used in this paper implies certain restrictive conditions regarding the physics of the problem, e.g., perfectly absorbing half-screens, plane wave propagation, $kr \gg 1$, and path difference approximations. However, as a mathematical function, its numerical evaluation may be accomplished even when the geometric parameters (h and r) tend to unrealistic physical values. For instance the use of partitioning provides valid answers for any knife-edge heights subject only to computer limitations. With regard to separation distances, the limitations are more inherent in the computational algorithm.

Mathematically, the MKE function can be evaluated for separation distances ranging from zero to infinity. This is apparent when closed form solutions of the function are available. For example, Vogler (1982) has derived the attenuation for three knife-edges under the condition $\theta_1 = \theta_2 = \theta_3 = 0$:

$$E/E_0 = (1/8)[1 + (2/\pi) \tan^{-1} a_1 + \tan^{-1} a_2 + \tan^{-1} a_3], \quad (37)$$

$$a_1 = [r_1(r_3+r_4)/r_2 r_t]^{1/2}, \quad a_2 = [(r_1+r_2)r_4/r_3 r_t]^{1/2},$$

$$a_3 = [r_1 r_4 / (r_2+r_3) r_t]^{1/2}, \quad r_t = r_1+r_2+r_3+r_4.$$

For r_2 or $r_3 = 0$, (37) reduces to the known expression for a double knife-edge. For r_2 and $r_3 = 0$, $(E/E_0) = 1/2$ which is the value for a single knife-edge.

When $r_2=r_3$ and r_1, r_4 take on various combinations of zero and infinity, (37) gives the same values as obtained from formulas in Lee (1978). In that paper the MKE attenuation for general N is derived under the conditions: all $\theta_i \equiv 0$; $r_2, \dots, r_N = \text{constant}$ (r_0 , say); and $r_1, r_{N+1} = 0$ or ∞ . Six cases are given which prove useful in helping to determine the validity of the computation series in the MKE computer program. The factor C_N (see equation (9)) is included in each case for purposes of later discussion.

Case (1): $r_1, r_{N+1} \rightarrow \infty$;

$$E/E_0 \sim 1/2, C_N \sim 0. \quad (38a)$$

Case (2): $r_1 \rightarrow \infty, r_{N+1} \rightarrow 0$ or $r_1 \rightarrow 0, r_{N+1} \rightarrow \infty$;

$$E/E_0 \sim \frac{1}{2} \frac{1 \cdot 3 \cdot 5 \cdots (2N-3)}{2 \cdot 4 \cdot 6 \cdots (2N-2)}, C_N \sim (1/2^{N-2})^{1/2}. \quad (38b)$$

Case (3): $r_1 = r_0, r_{N+1} \rightarrow 0$ or $r_1 \rightarrow 0, r_{N+1} = r_0$;

$$E/E_0 \sim 1/2N, C_N \sim (N/2^{N-1})^{1/2}. \quad (38c)$$

Case (4): $r_1, r_{N+1} \rightarrow 0$;

$$E/E_0 \sim 1/4(N-1), C_N \sim [(N-1)/2^{N-2}]^{1/2}. \quad (38d)$$

Case (5): $r_1, r_{N+1} = r_0$;

$$E/E_0 \sim 1/(N+1), C_N = [(N+1)/2^N]^{1/2}. \quad (38e)$$

Case (6): $r_1 \rightarrow \infty, r_{N+1} = r_0$ or $r_1 = r_0, r_{N+1} \rightarrow \infty$;

$$E/E_0 \sim \frac{1 \cdot 3 \cdot 5 \cdots (2N-1)}{2 \cdot 4 \cdot 6 \cdots (2N)}, C_N \sim (1/2^{N-1})^{1/2}. \quad (38f)$$

Comparisons of attenuation for N=10 as calculated from (38) and as calculated from program PAMKE are shown in Table 1. The values used in PAMKE when r_1, r_{11} approached 0 or ∞ were 10^{-9} or 10^8 , respectively; in all cases r_0 was set equal to unity.

Table 1. Attenuation Comparisons for N=10

<u>Case</u>	<u>E/Eo(equat.(38))</u>	<u>E/Eo(PAMKE)</u>	<u>C₁₀</u>
(1)	0.5000	~0	0
(2)	0.09274(20.66dB)	0.08639(21.27dB)	0.0625
(3)	0.05000(26.02dB)	0.04998(26.02dB)	0.1398
(4)	0.02778(31.13dB)	0.02778(31.13dB)	0.1875
(5)	0.09091(20.83dB)	0.09076(20.84dB)	0.1036
(6)	0.1762(15.08dB)	0.1551(16.19dB)	0.0442

The maximum number of series terms (160) was used in all cases for the PAMKE calculations. When C_N is close to zero, this number of terms is insufficient to provide a valid answer. In cases (2) and (6) the result is good to about one significant figure; however, in cases (3), (4), and (5) PAMKE gives three or more significant figures.

The factor C_N Provides a good indication as to how closely the series calculation approaches the correct answer. Table 1 suggests (and other studies tend to verify) that for $C_N \gtrsim 0.1$, the attenuation is good to about 0.1 dB or better; as C_N ranges below 0.1, the accuracy becomes poorer. Note that the C_N in (38) increase as N decreases, which should result in better accuracy. Cases (2) and (6) were run for N's such that $C_N=0.125$ in each case. For case (2) (N=8), PAMKE gave $(E/E_0)=0.1037$ as against an exact value of 0.1047; for case (6) (N=7), PAMKE gave $(E/E_0)=0.2073$ versus the exact value 0.2095. The difference in dB in each case is about 0.09 dB.

The condition, all θ 's=0, is a "worst case" situation as far as series convergence within a set number of terms is concerned. This is because repeated integrals of the error function decrease rapidly as the argument β increases, and fewer terms are required to assure a given number of significant figures. This fact, combined with the partitioning procedure, means that the relationship, $C_N \gtrsim 0.1$, provides a fairly conservative accuracy test for PAMKE when applied to most propagation paths.

If each and every diffraction angle θ_i is large enough such that every $\beta_i \gg 1$, then the attenuation is well approximated by the first term of the series expansion derived in the original MKE paper:

$$E/E_0 \sim 2^{-N} C_N e^{\sigma_N - \sigma'_N} \prod_{i=1}^N \operatorname{erfc}(\beta_i), \quad (39)$$

where $\operatorname{erfc}(z)$ is the complementary error function as defined in Abramowitz and Stegun (1964;p.297). Since $\beta_i \gg 1$ for $i=1, \dots, N$, $\operatorname{erfc}(\beta_i)$ may be replaced by the first term of its asymptotic expansion and (39) then becomes

$$\begin{aligned} E/E_0 &\sim (2\sqrt{\pi})^{-N} C_N e^{-\sigma'_N} / \beta_1 \dots \beta_N \\ &= e^{-\sigma'_N} (i2\pi k)^{-N/2} (R_{N+1}/r_1 \dots r_{N+1})^{1/2} / \theta_1 \dots \theta_N, \end{aligned} \quad (40)$$

where R_{N+1} denotes the total path distance, σ'_N is defined in (26), and use has been made of (2), (9), (21), and (27).

Equation (40) is of interest in that it may also be obtained from the Geometrical Theory of Diffraction (GTD). If the knife-edge configuration is such that each edge lies well into the shadow region of the preceding knife-edge, the GTD diffracted field can be expressed as the product of functions of the form

$$f(s) = s^{-1/2} e^{-iks}, \quad (41a)$$

$$D(\epsilon, \delta) = (2\sqrt{2\pi k})^{-1} \left[\csc \left\{ (\delta + \epsilon)/2 \right\} \pm \sec \left\{ (\delta - \epsilon)/2 \right\} \right] e^{-i\pi/4}. \quad (41b)$$

In the above, s is the slant distance to the edge, ϵ and δ are the elevation angles as measured from the horizontal to the top of the knife-edge at the source and at the field point, respectively, and the plus or minus signs in the Keller diffraction coefficient D correspond to vertical or horizontal polarization (Keller, 1962).

Since $(\epsilon + \delta) = \theta$, the diffracted field u_d for a single knife-edge according to the GTD is

$$\begin{aligned} u_d &= f(s_1) D(\theta_1) f(s_2) \\ &\sim (e^{-iks_1} / \sqrt{s_1}) \left[\sqrt{i2\pi k} \theta_1 \right]^{-1} (e^{-iks_2} / \sqrt{s_2}), \end{aligned} \quad (42)$$

where the approximate expression is valid for

$$0 \ll \theta_1 \text{ and } \theta_1 \approx \sin \theta_1 \quad . \quad (43)$$

In the case of multiple knife-edges, the diffracted field is the product of functions, $D(\theta_i)f(s_{i+1})$:

$$u_d = f(s_1)D(\theta_1)f(s_2) \dots D(\theta_N)f(s_{N+1}) \\ \sim (i2\pi k)^{-N/2} e^{-ik(s_1 + \dots + s_{N+1})} \left\{ (s_1 \dots s_{N+1})^{1/2} \theta_1 \dots \theta_N \right\}^{-1} , \quad (44)$$

$$0 \ll \theta_i \text{ and } \theta_i \approx \sin \theta_i, \quad i = 1, \dots, N. \quad (45)$$

For a reference free-space field, $R_{N+1}^{-1/2} \exp(-ikR_{N+1})$, and assuming $s_i \approx r_i$ except in the phase term where use is made of the approximation in (3), we see that the GTD attenuation obtained from (44) is identical to (40).

Two widely used approximations to MKE diffraction have been suggested by Epstein and Peterson (1953) and by Deygout (1966). Both approximations consist simply of products of single knife-edge attenuation functions, the difference being in the way the "source" and "receiver" of each knife-edge are determined. If we designate the single knife-edge function as given in (28) by: $A_S(\beta) = (1/2)\text{erfc}(\beta)$, the Epstein-Peterson (A_{EP}) and Deygout (A_D) approximations can be expressed as

$$A_{EP} = \prod_{m=1}^N A_S(\beta_m) , \quad A_D = \prod_{m=1}^N A_S(\beta'_m) , \quad (46)$$

where β_m is defined in (21) and β'_m has the same form but with the distances and diffraction angle θ'_m determined from Deygout's "principle mask" method.

Pogorzelski (1982) has pointed out that, under the conditions (45) where the GTD equation (40) is valid, A_{EP} has the same θ dependence but the r and the phase dependence differs; A_D has the same r and phase dependence but the θ dependence is different. Thus, asymptotic expressions for the two approximations are

$$A_{EP} \sim e^{-\sigma_N} (i2\pi k)^{-N/2} F_{EP}(r) / \theta_1 \dots \theta_N, \quad (47a)$$

$$F_{EP}(r) = \begin{cases} [(r_1+r_2)\dots(r_N+r_{N+1})/r_1(r_2\dots r_N)^2 r_{N+1}]^{1/2}, & N \geq 2 \\ 1/\rho_1, & N = 1 \end{cases}$$

$$A_D \sim e^{-\sigma'_N} (i2\pi k)^{-N/2} F_D(r) / \theta'_1 \dots \theta'_N, \quad (47b)$$

$$F_D(r) = [R_{N+1}/r_1 \dots r_{N+1}]^{1/2}.$$

The difference in dB between the approximations and (40), assuming (45), can be written as

$$(A_{EP})_{dB} \sim (E/E_0)_{dB} - 20 \log(1/C_N), \quad (48a)$$

$$(A_D)_{dB} \sim (E/E_0)_{dB} + 20 \log(K_1 \dots K_N), \quad (48b)$$

$$\theta'_m = K_m \theta_m, \quad m=1, \dots, N.$$

Figure 4 compares some of the attenuation formulas discussed in this section. The propagation path is the same as that assumed for Figure 3, i.e., five evenly spaced knife-edges with heights simultaneously varying such that all θ 's are equal to the same value. The attenuation in dB is plotted versus this value, θ in mrad, for the MKE function (from program PAMKE), the GTD (from equation (40)), and the two approximations from (46), A_{EP} and A_D .

As expected, the MKE and GTD give the same result for $\theta \gtrsim 0.015$ rad. Of course, for very large θ the two curves begin to diverge, with the GTD being exact and the MKE an approximation. For θ decreasing to zero, no GTD formula for five knife-edges exists at the present time and the approximation of (40) is not valid in this region. In fact at $\theta=0$, the attenuation has the value, $-20 \log(1/6)=15.56$ dB (see equation (38e)), whereas (40) goes to $-\infty$.

The Epstein-Peterson and Deygout approximations both have the value $5(6.02)=30.1$ dB at $\theta=0$, which exceeds the exact value by 14.5dB. When $\theta \gg 0$, A_{EP} and A_D approach constant differences from the exact curve as is indicated in (48). For A_{EP} the difference is $20 \log(1/C_5)=7.27$ dB; for A_D the difference is equal to $20 \log[3(3/2)(3/2)]=16.6$ dB.

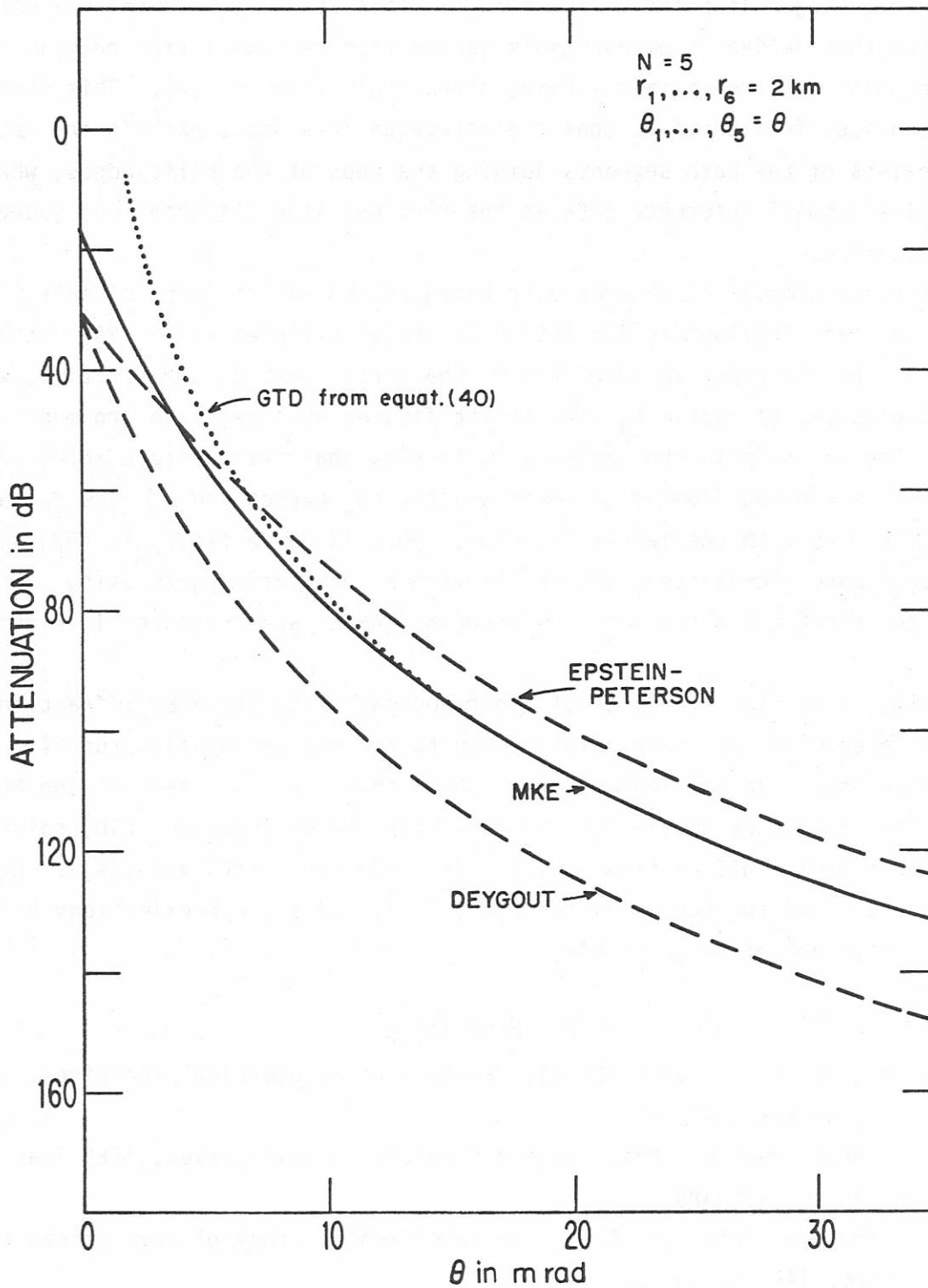


Figure 4. Attenuation for the same five knife-edge path as in Figure 3 (all θ 's equal). Comparisons are shown for MKE, GTD, and the approximations of Epstein-Peterson and of Deygout.